Numerical evaluation of x-mode beam broadening at plasma edge using a FDTD fullwave code

F. da Silva[1], S. Heuraux[2], E. Sysoeva[3], E. Gusakov[3], A. Popov[3]

[1] *Instituto de Plasmas e Fusão Nuclear, Instituto Superior Técnico, Universidade de Lisboa, 1049-001 Lisboa, Portugal*

[2] *Institut Jean Lamour, UMR 7198 CNRS-University of Lorraine, Vandœuvre, France*

[3] *Ioffe Institute, 194021 Politekhnicheskaya st 26, St Petersburg, Russia*

Abstract

Microwave beams are commonly used in fusion plasma machines either for diagnose, such as in reflectometry or Collective Thomson Scattering, or for heating purposes being ECRH an example of it. In this work we look into the broadening of the width of probing beam for the case of extraordinary mode propagation in turbulent inhomogeneous plasma for different turbulence k-spectra and plasma conditions using a 2D fullwave finite-difference time-domain code.

Introduction

The width and positioning of the probing play an important role in reflectometry, namely in wave number selection. It is also important for heating systems for having an efficient deposition of power. Consequently it is an important contemporary topic of research since high levels of edge turbulence and long plasma paths are expected in future fusion machines such ITER, a fact that lead to several works dealing with the enlargement of ordinary mode probing beams, either numerical [3, 1] (reflectometry) or analytical [2] (ECRH). The ECRH studies reach conclusions that are also relevant for reflectometry. We propose to extend these studies on beam behavior to the X-mode using a 2D FDTD full-wave code, REFMULX. The code has two kernels implemented, a classic discretization, the Xu-Yuan kernel (XYK)[4] with modifications (MXYK) and a new innovative energy conservative kernel, proposed by B. Després and M. Campos Pinto, the Després-Pinto kernel (DPK) [5], which changes time centering of **J** and relates **J** and **E** in a Crank-Nicolson way. These kernels' algorithms are different and can be used to crosscheck the results. With plasma movement, a correction is formally needed to the **J** PDE and has been included in the DPK. The weight of the correction will depend on $\partial_t n_e$ and can be either important or negligible. The present results with DPK with and without correction are very similar implying that the correction plays a minute role. It also assures that the use of Xu-Yuan kernel is valid (no correction on **J** is yet implemented on XYK).

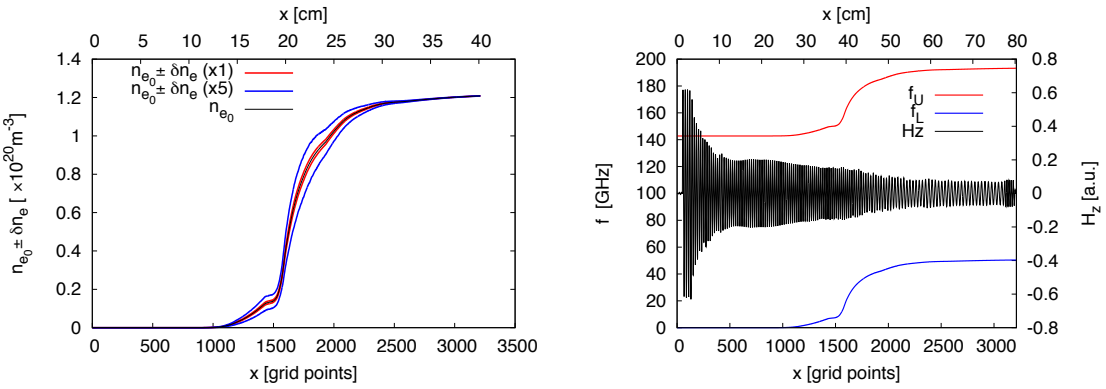

(a) Density profile.

(b) Frequency access and axial cut of H_z.

Figure 1: On the left the density profile n_e used is shown in black. Around n_e the RMS envelopes for the added turbulence for the lowest and the highest levels used. On the right the frequency access shows that for a frequency of $f_c = 60\,\text{GHz}$ the wave traverses the plasma *between* the upper and lower frequencies cutoffs.

Numerical Simulation and results

The approach to this work follows the one used in [2]. We use a plasma slab model with 2400×1900 grid points ($60 \times 47.5\,\text{cm}$). The size of the grid is 3212×1900 grid points ($80.3 \times 47.5\,\text{cm}$)—The extra 20.3 cm account for vacuum. A radial density profile, compatible with ITER, was chosen (see Fig. 1a) and probed with a frequency $f_c = 60\,\text{GHz}$. For this value of f_c no cutoff present and the probing beam propagates *above* lower cutoff as observed in Fig. 1b. The number of iterations on each run was $322,240$ iterations and for higher statistics averages of several runs were used. For a given amplitude $A(i,j)$ and a random phase $\varphi(i,j)$, a turbulence scenario can be build using Fourier synthesis (calculated with IFFT). Long poloidal turbulence matrices ($L_y = 17,640\,\text{gridpoints} = 4.41\,\text{m}$) cycle through the grid with a poloidal velocity $V_{pol}/c = 10\%$. Also as a given input to the problem is the radial density fluctuation profile. The beam is constructed from several poloidal cuts of the field H_z at different radial positions which are integrated on time $\int |H_z|^2 \mathrm{d}t$. This gives a spatial distribution (mapping) of the probing wave density power. Even in the presence of turbulence where the probing beam may be split in several sub-beams at each instant, there will be an average localization of the power deposition correlating with this integrated beam. Running with vacuum the characteristics of the injected beam can be obtained, namely its half-power width. The beam is injected along the antenna axis perpendicular to the plasma. With plasma and a magnetic field $B_0 = +5.1\,\text{T}$ without turbulence ($\delta n_e = 0$) a deviation and enlargement of the beam is noticed. The strong density gradient is at the origin of this deflection [6] and it is put in evidence by experimenting with differ-

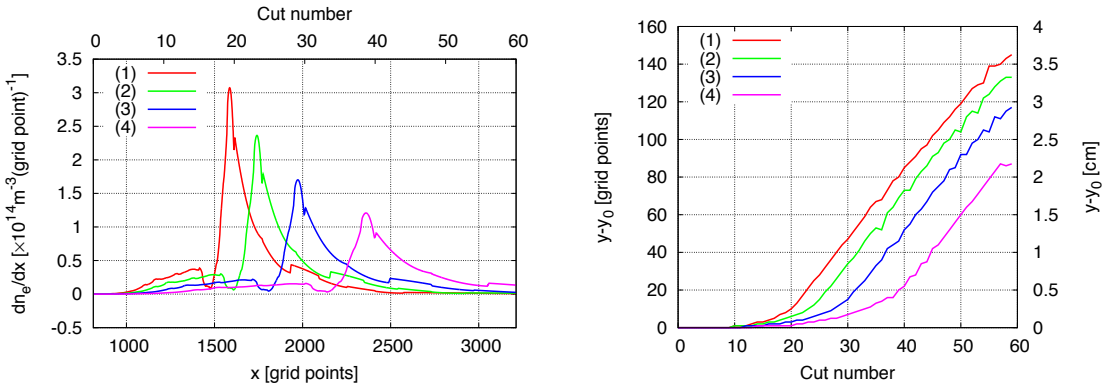

(a) Density gradients $\partial n_e/\partial x$

(b) Position of the maxima of the integrated beam.

Figure 2: The position where density gradients jump up correlate with the augmentation of the deviation suffered by the beam. Density gradient (1) corresponds with the profile displayed in Fig. 1a

ent density gradients $\partial n_e/\partial x$ as shown in Fig. 2a. The maxima of the deflected beams are displayed on Fig. 2b. Reversing the sign of the magnetic field $B_0 = -5.1\,\mathrm{T}$ a change in the direction of the deviation is observed. The value of the maxima is slightly lower though. To notice that both kernels give equivalent consistent results conferring a validation of them. Turbulence adds to the degradation of the beam enlarging it and deviating the position of the maxima. In order to obtain better statistics results were build using an average from 7 runs from different realizations of turbulence matrices making it *equivalent* to $2,255,680$ *iterations* assuming ergodicity.

Conclusions

Direction of the turbulence velocity plays a role in enlargement of the beam. The results are important to help understand behavior of a probing beam having applications to reflectometry, in selection of wavenumber, probing path and on the effective spot of the beam. Also for uses in power systems for the correct deposition of power. These simulations raise interesting points for follow up work such as the role of the density gradients at the edge (similar to those found in ITER), the impact of turbulence (spectra, radial distribution), the magnetic field bias and the influence of the direction of turbulence flow. Both kernels give consistent results.

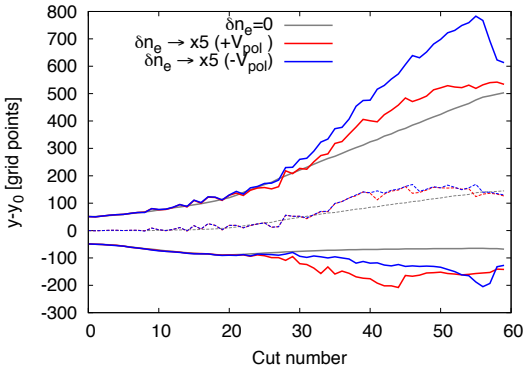

(a) Half width power for $B_0 = +5.1\,\mathrm{T}$.

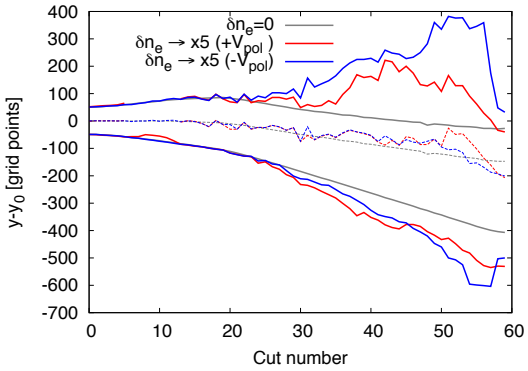

(b) [Half width power for $B_0 = -5.1\,\mathrm{T}$

Figure 3: Half-power widths of the integrated beams with positive and negative magnetic field B_0. The broken lines show the position of the beams' maxima while the continuous lines show the position of the half-power width at each side of the maxima. The *positive* direction of the turbulence flow is displayed in red ($+V_{pol}$) while the *negative* ($-V_{pol}$) in blue. For reference the beam without turbulence appears in grey.

Acknowledgements

IPFN activities received financial support from *Fundação para a Ciência e Tecnologia* through project UID/FIS/50010/2013. UL activities received support from ANR CHROME ANR-12-BS0006-01.

References

[1] F. da Silva, S. Heuraux, E. Gusakov, A. Popov, Proc. 11th Intl. Reflectometry Workshop for fusion plasma diagnostics — IRW11 (Padova, May, 2011).

[2] E. Sysoeva, F. da Silva, E. Gusakov, S. Heuraux, A Popov, Nuclear Fusion, **55** (2015).

[3] F. da Silva, S. Heuraux, E. Gusakov, M. Manso and A. Surkov, Proc. 8th Intl. Reflectometry Workshop for fusion plasma diagnostics — IRW8 (St Petersburg, May, 2007).

[4] Lijun Xu, Naichang Yuan, IEEE Antennas And Wireless Propagation Letters **5**, 335–338 (2006).

[5] Filipe da Silva, Martin Campos Pinto, Bruno Després, Stéphane Heuraux, Journal of Computational Physics **295** (2015) 24–45.

[6] R. B. White and F. F. Chen, Plasma Physics **16** (1974) 565.